J Mol Model (2011) 17:1017–1027
DOI 10.1007/s00894-010-0799-0

ORIGINAL PAPER

Nitrosation of malononitrile by HONO, ClNO and N_2O_3: A theoretical study

Kun Yang · Xiao-Fang Chen · Jian-Yong Liu · Wei-Peng Lai · Bo-Zhou Wang

Received: 10 October 2009 / Accepted: 6 July 2010 / Published online: 22 July 2010

Abstract Nitrosation reactions of malononitrile by three nitrosating agents, HONO, ClNO, and N_2O_3, have been theoretically investigated at the B3LYP/cc-pVTZ and MP2/cc-pVDZ levels. Two possible competitive paths for nitrosation of malononitrile to give 2-nitroso-malononitrile were proposed: (a) direct C-nitrosation and (b) N-nitrosation and subsequent nitroso transfer from N to C atom. The calculations show that at both B3LYP and MP2 levels, path b is kinetically favored over path a for nitrosations by HONO and N_2O_3. In the case of ClNO, the B3LYP predicts preference of path b, while the MP2 calculations suggest that both paths have similar rate-determining barriers. The data suggest that N_2O_3 is the preferred nitrosating agent for the nitrosation of malononitrile in aqueous solution. Transformation of 2-nitroso-malononitrile to form malononitrileoxime via intramolecular proton transfer has also been explored, and it is found that inclusion of an assistant water molecule can drastically accelerate the tautomerization.

Keywords Malononitrile · Nitrosation · Nitroso transfer · Reaction mechanism

K. Yang · X.-F. Chen · J.-Y. Liu (✉)
State Key Laboratory of Molecular Reaction Dynamics,
Dalian Institute of Chemical Physics,
Chinese Academy of Sciences,
Dalian 116023, China
e-mail: beam@dicp.ac.cn

W.-P. Lai · B.-Z. Wang
Xi'an Modern Chemistry Research Institute,
Xi'an 710065, China

Introduction

Nitrosation reactions [1] play important roles in many areas of chemistry. For example, due to the ability to generate toxic and carcinogenic N-nitrosamines [2], nitrosation reactions have aroused much interest in biological chemistry [3, 4]. Nitrosation reactions are also related to the chemical, petroleum, and explosives industries.

Malononitrile (1, Scheme 1) is a highly reactive compound undergoing a rich and varied chemistry [5]. It has been widely used as a starting material or reaction intermediate since its methylene group and either one or both nitrile groups can participate in condensation reactions in the synthesis of addition products and heterocyclic compounds [6–8]. In the laboratory, the nitrosation of malononitrile under aqueous acidic conditions leads to the formation of malononitrileoxime (4, Scheme 1) [9–11], which can be used as a precursor material in the synthesis of nitrogen-rich compounds [11, 12]. However, no theoretical investigations on the nitrosation mechanism of malononitrile have been carried out to the best of our knowledge.

In this work, we have concentrated on the nitrosation chemistry of malononitrile to give a theoretical insight into the reaction mechanism. Three nitrosating agents of the form XNO, where X is a strong nucleophilic species, were taken into account. The first nitrosating agent is nitrous acid, HONO. The second one is nitroso chloride, ClNO, which is formed by the reaction of HONO with hydrochloric acid (Eq. 1), a commonly used acid in the nitrosation of malononitrile [11, 13]. The third nitrosating agent considered here is dinitrogen trioxide, N_2O_3, which is obtained by the dehydration between two HONO molecules (Eq. 2). Theoretical elucidation of the formation of ClNO [14] and N_2O_3

Scheme 1 Possible paths for nitrosation of malononitrile, 1

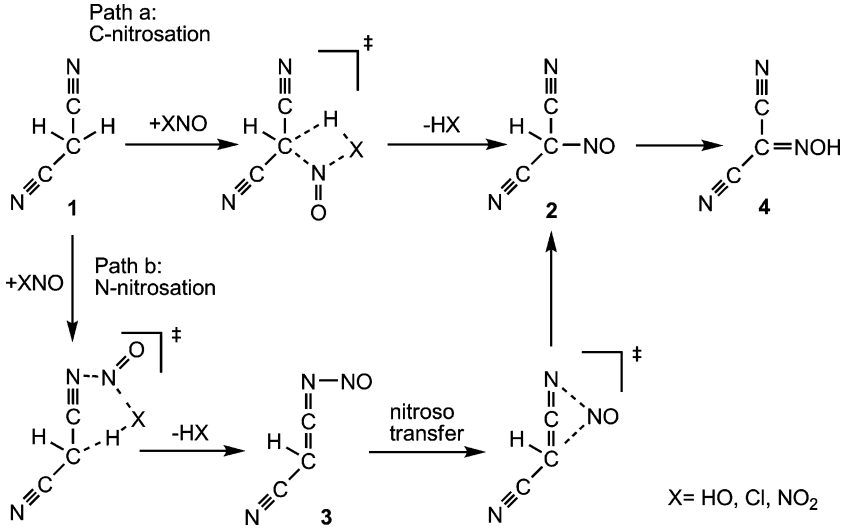

[15, 16] have been previously reported. In our calculations, we have focused on the nitrosation mechanisms.

$$HONO + HCl \rightarrow ClNO + H_2O \quad (1)$$

$$2HONO \rightarrow N_2O_3 + H_2O \quad (2)$$

Nitrosation of malononitrile proceeds through initial formation of C-nitroso species, 2-nitroso-malononitrile (2, Scheme 1). We proposed two mechanistic possibilities to give 2-nitroso-malononitrile, leading from malononitrile with nitrosating agents, as shown in Scheme 1. For the first path, path a, there is a direct attack of the nitroso of nitrosating agent on the methylene carbon atom of malononitrile to give 2-nitroso-malononitrile, 2, with an HX molecule. The second path, path b, is a stepwise process, beginning with the nitroso of nitrosating agent attacking on the nitrile nitrogen atom of malononitrile to generate the N-nitroso species, 3, with an HX molecule. Subsequent intramolecular N → C nitroso transfer then derives the N-nitroso species, 3, to 2-nitroso-malononitrile, 2. Our main purpose of this work is to present theoretical knowledge of the transition states and free energy barriers for the nitrosations of malononitrile, to investigate the two mechanistic possibilities, to compare the nitrosating capabilities of the three nitrosating agents, and to make a reliable assessment of their roles in the nitrosating reaction. We have also explored the energetics for the tautomerization of 2-nitroso-malononitrile, 2, to malononitrileoxime, 4, in an effort to explain the experimentally observed product.

Computational details

All the minimum and transition state geometries were located using both the B3LYP hybrid functional [17, 18] with the cc-pVTZ basis sets [19, 20] and the second-order Møller − Plesset perturbation theory [21] with the cc-pVDZ basis sets [19, 20] as implemented in the Gaussian 03 program package [22]. Vibrational frequency calculations were performed to confirm that the transition state structures presented one imaginary frequency, whereas the minimum energy structures had only real frequencies. Intrinsic reaction coordinate (IRC) [23, 24] pathways were traced to verify the connectivity between minima and associated transition states. The natural population analysis (NPA) of charge was performed by the natural bond orbital (NBO) analysis [25–29] using the NBO 3.1 program [30] in Gaussian 03 at the MP2/cc-pVDZ level. Since the experimental studies of the nitrosation of malononitrile were carried out in aqueous solution [9–11], the effect of solvent medium was investigated at both the B3LYP and the MP2 levels using the polarizable continuum model (PCM) [31] applying the dielectric constant of water (ε=78.39) at their corresponding gas phase optimized geometries. All free energies reported were calculated under standard conditions (298.15 K and one atmosphere), with the thermal correction of Gibbs free energy in the gas phase. All the calculations have been done with Born-Oppenheimer approximation since in most cases this approximation can describe chemical reaction very well [32–36].

Results and discussion

Nitrosation of malononitrile by HONO

Nitrous acid, HONO, is known to bear *trans* and *cis* isomers (Fig. 1) with competing stability [1, 37]. Both *trans*- and *cis*-HONO were considered as the nitrosating agents in the calculation. Figure 2 shows the computed energetics and the optimized geometries of the reactants,

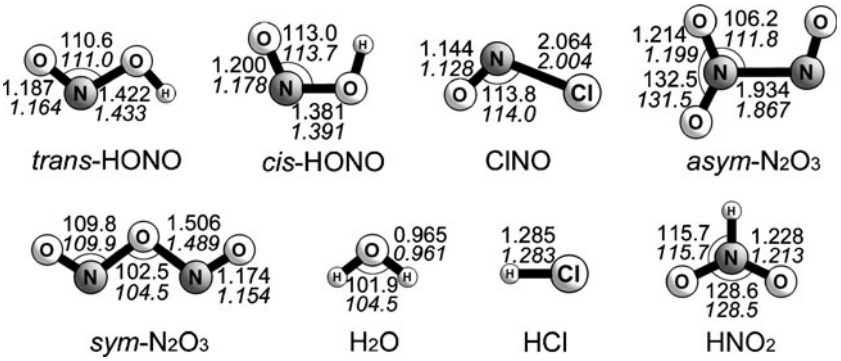

Fig. 1 Optimized geometries of the nitrosating agents (HONO, ClNO, and N_2O_3), H_2O, HCl and HNO_2 at the MP2/cc-pVDZ (numbers in regular form) and B3LYP/cc-pVTZ (numbers in italics) levels. Bond lengths are in angstroms, and angles are in degrees

transition states and products for the nitrosation of malononitrile, 1, by HONO. The energy profiles in Fig. 2a involve an initial complex formation, CP1, between malononitrile and *trans*-HONO, followed by either C- or N-nitrosation reaction. At the MP2/cc-pVDZ level, a free energy barrier of 36.5 kcalmol^{-1} is predicted for the C-nitrosation reaction (path a, TS1) in the gas phase, where the nitroso of *trans*-HONO attacks on the methylene carbon atom of malononitrile, while an H transfers from malononitrile to the hydroxyl group of *trans*-HONO. The NPA charge of the transferred H is calculated to be 0.515, indicating that it is more like a proton than a hydrogen transfer. This C-nitrosation reaction leads to the formation of 2-nitroso-malononitrile, 2, with a water molecule, and the reaction is slightly endothermic by 1.9 kcalmol^{-1}. At the B3LYP/cc-pVTZ level, however, no transition structure with TS1 conformation could be found.

For the N-nitrosation transation state TS2, the nitroso group of *trans*-HONO attacks onto the nitrile nitrogen of malononitrile with an H transfer from malononitrile to the hydroxyl group of *trans*-HONO, leading to the generation of N-nitroso species, 3, and a water molecule. The calculated NPA charge of the transferred H in TS2 is 0.529, also more like a proton transfer. The free energy barrier of TS2 at the MP2 level is 31.9 kcalmol^{-1} in the gas phase, which is 4.6 kcalmol^{-1} preferred in energy than that for the C-nitrosation (TS1, 36.5 kcalmol^{-1}). Similar barrier of 34.8 kcalmol^{-1} for TS2 is predicted at the B3LYP/cc-pVTZ level. However, the formation of 3+H_2O undergoes a much stronger endothermic reaction (21.1 kcalmol^{-1}) with respect

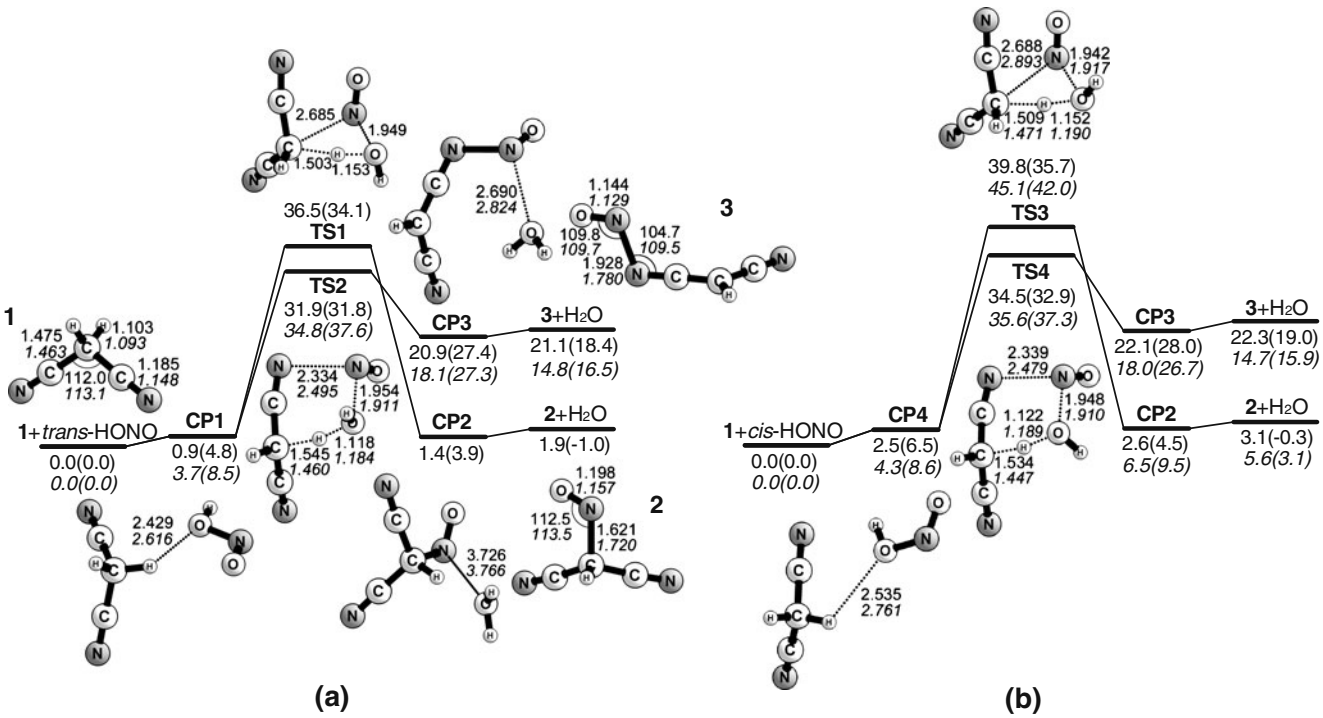

Fig. 2 Free energy profiles for the nitrosation of malononitrile, 1, by HONO in the gas phase (in kcalmol^{-1}) at the MP2/cc-pVDZ (numbers in regular form) and B3LYP/cc-pVTZ (numbers in italics) levels. Numbers in parentheses are the relative free energies in water solvent

to the formation of 2+H_2O (1.9 kcalmol^{-1}). These results indicate that though the C-nitrosation is thermodynamically favored over the N-nitrosation, the N-nitrosation reaction is kinetically more preferable. The preference for initial N-nitrosation can be understood as reflecting the reduction in ring strain of the transition states. In path a, transition state TS1 holds a strained four-membered ring structure, whereas in path b, TS2 is a less strained six-membered ring transition state, leading to the lower activation barrier.

Figure 2b shows the free energy profiles for the nitrosation reactions by *cis*-HONO. Similar to the NPA calculations in TS1 and TS2, the NPA charges obtained for the transferred H in TS3 and TS4 are 0.519 and 0.531, respectively, indicating the proton transfer nature. The free energy barrier for the N-nitrosation (TS4) is predicted to be 34.5 (35.6) kcalmol^{-1} in the gas phase at the MP2/cc-pVDZ (B3LYP/cc-pVTZ) level, which is 5.3 (9.5) kcalmol^{-1} lower than that for the C-nitrosation transition state TS3, also suggesting the preference for the N-nitrosation mechanism.

The inclusion of solvent effect of water, through the continuum model, has also been studied. As shown in Fig. 2, at the MP2/cc-pVDZ level, the solvent effect lowers all free energy barriers but by small amount of 0.1~4.1 kcalmol^{-1}. At the B3LYP/cc-pVTZ level, the solvent effect slightly decreases the barrier of TS3 by 3.1 kcalmol^{-1} and slightly increases the barriers of TS2 and TS4 by 2.8 and 1.7 kcalmol^{-1}, respectively. However, water may play an additional explicit role in catalyzing the reaction. Therefore, we explored the possible role of an assistant water molecule in the nitrosation reactions of malononitrile by HONO.

The energy profiles for the water-assisted nitrosations of malononitrile by HONO are shown in Fig. 3, together with the optimized geometries. Two transition states, TS2′ and TS4′, which are the water-assisted transition states for the N-nitrosation of malononitrile by *trans*-HONO (TS2) and *cis*-HONO (TS4), respectively, were found. All efforts to locate the water-assisted transition states for the C-nitrosation of malononitrile by *trans*-HONO (TS1) or *cis*-HONO (TS3) were unsuccessful. As shown in Fig. 3, the presence of the assistant water molecule little influences the gas phase free energy barriers, which are predicted to be 33.5 (37.7) kcalmol^{-1} for TS2′ and 34.1 (38.9) kcalmol^{-1} for TS4′ at the MP2/cc-pVDZ (B3LYP/cc-pVTZ) level, respectively. Further inclusion of the solvent effect, however, leads to the increase of the barriers to 39.0 (46.9) and 41.3 (47.9) kcalmol^{-1} for TS2′ and TS4′ at the MP2/cc-pVDZ (B3LYP/cc-pVTZ) level, respectively, suggesting the disadvantage of the water-assisted nitrosation mechanism in aqueous solution. Therefore, our calculations indicate that for the nitrosation of malononitrile by HONO in aqueous solution, water has non-catalyst character, but only serves as solvent.

Nitrosation of malononitrile by ClNO

The optimized geometrical structures and energetics for the nitrosation of malononitrile, 1, by ClNO are shown in Fig. 4. Both paths a and b start with the initial formation of the complex, CP5, which lies 1.8 and 5.2 kcalmol^{-1} above its separated components in the gas phase at the MP2/cc-pVDZ and B3LYP/cc-pVTZ levels, respectively. The direct C-nitrosation of malononitrile by ClNO proceeds over a four-membered ring transition state TS5 with an energy barrier of 34.9 kcalmol^{-1} in the gas phase at the MP2/cc-pVDZ level, and the resulting formation of 2 with an HCl molecule is endothermic by 6.5 kcalmol^{-1} with respect to the reactants. At the B3LYP/cc-pVTZ level, a much larger barrier of

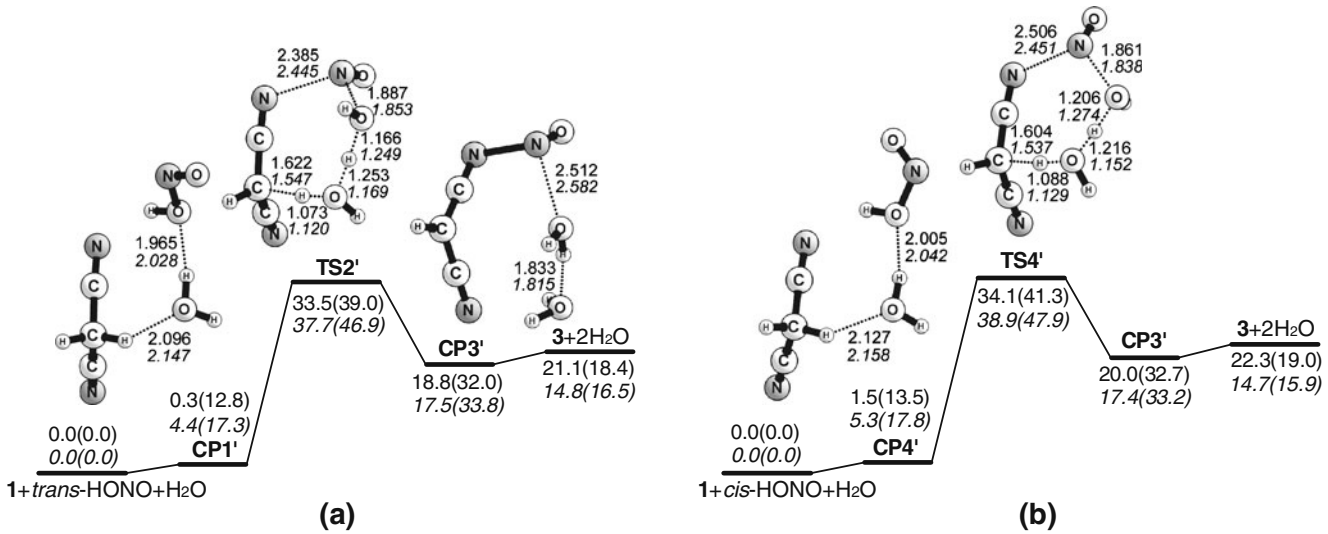

Fig. 3 Free energy profiles for the water-assisted nitrosation of malononitrile, 1, by HONO in the gas phase (in kcalmol^{-1}) at the MP2/cc-pVDZ (numbers in regular form) and B3LYP/cc-pVTZ (numbers in italics) levels. Numbers in parentheses are the relative free energies in water solvent

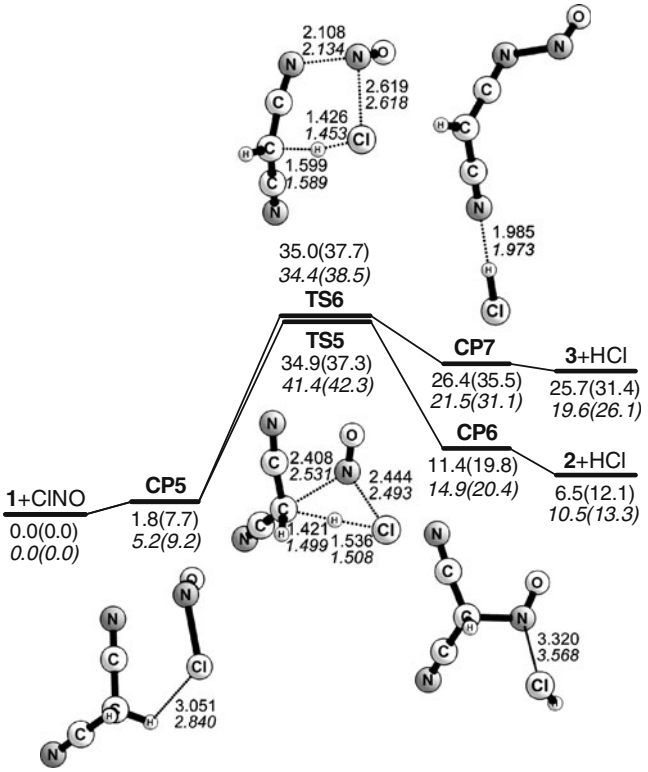

Fig. 4 Free energy profiles for the nitrosation of malononitrile, 1, by ClNO in the gas phase (in kcalmol^{-1}) at the MP2/cc-pVDZ (numbers in regular form) and B3LYP/cc-pVTZ (numbers in italics) levels. Numbers in parentheses are the relative free energies in water solvent

41.4 kcalmol^{-1} is obtained, which is 6.5 kcalmol^{-1} higher than that obtained at the MP2/cc-pVDZ level. This barrier height difference brought about by the two methods seems attributed to the different transition structure behaviors. The MP2 predicted distance between the C atom and the transferred H atom of transition state TS5 is 1.421 Å, which is ~0.08 Å smaller than that obtained at the B3LYP level (1.499 Å). This smaller C···H distance indicates that this transition structure at the MP2 level appears to be late compared to the B3LYP obtained transition state. Therefore, transition state TS5 at the MP2 level resembles a little bit closer to the stable complex CP5 rather than the less stable complex CP6, presenting a relatively lower barrier height.

For path b, the MP2/cc-pVDZ level predicts that the free energy barrier for the N-nitrosation transition state TS6 (35.0 kcalmol^{-1}) is almost the same as that of TS5, indicating essentially identical preference for both C- and N-nitrosations by ClNO. The free energy barrier obtained at the B3LYP/cc-pVTZ level for TS6 (34.4 kcalmol^{-1}), however, is 7.0 kcalmol^{-1} lower than that of TS5, suggesting the kinetical preference of N-nitrosation. The NPA charges of the transferred H in TS5 and TS6 are 0.335 and 0.347, respectively. Therefore, these H transfers are also proton rather than hydrogen transfers. Solvent effect appears to have unfavorable influence over the calculated energetics: the activation barriers are slightly increased, and the reactions become more endothermic at both the MP2 and B3LYP levels.

The energetics of the water-assisted nitrosations of malononitrile by ClNO were also calculated, which are presented in Fig. 5, together with the optimized geometries. It is found that inclusion of an assistant water molecule slightly increases the gas phase activation barriers by 3.0 (2.3) and 0.2 (1.0) kcalmol^{-1} for TS5′ and TS6′ at the MP2/cc-pVDZ (B3LYP/cc-pVTZ) level, respectively. Additional involvement of solvent effect further increases the barrier heights, similar to the trend found in the case of nitrosations by HONO. This suggests that in water solution, the nitrosation reaction by ClNO would also proceed in a nonwater-assisted mechanism.

Nitrosation of malononitrile by N_2O_3

For dinitrogen trioxide, N_2O_3 (Fig. 1), two isomers are identified, namely *asym*- and *sym*-N_2O_3 [38, 39], and the *asym* isomer is thought to be more stable. Both these two N_2O_3 isomers were considered in the nitrosating processes.

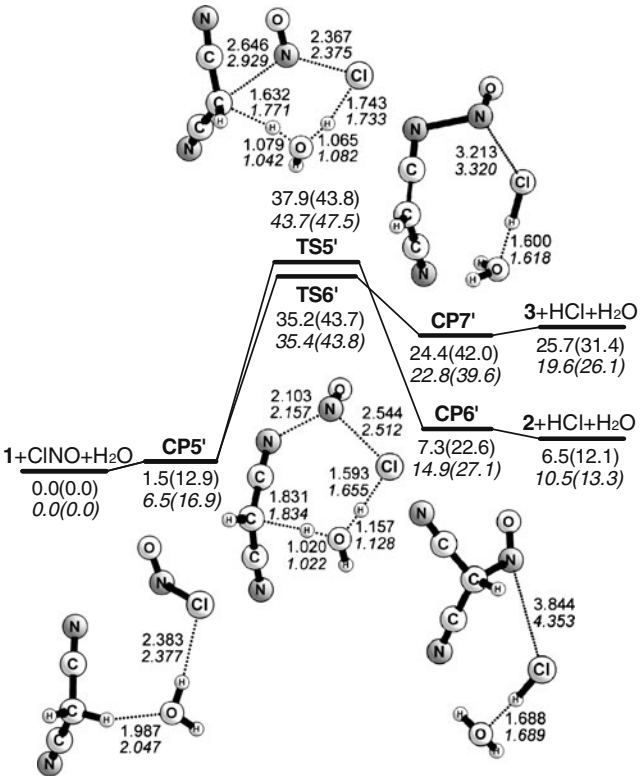

Fig. 5 Free energy profiles for the water-assisted nitrosation of malononitrile, 1, by ClNO in the gas phase (in kcalmol^{-1}) at the MP2/cc-pVDZ (numbers in regular form) and B3LYP/cc-pVTZ (numbers in italics) levels. Numbers in parentheses are the relative free energies in water solvent

Figure 6 shows the optimized geometries and the energetics for the nitrosations of malononitrile by *asym*- and *sym*-N_2O_3, with energy values referring to 1+*asym*-N_2O_3 (Fig. 6a), and 1+*sym*-N_2O_3 (Fig. 6b), respectively.

Totally six transition states, TS7-TS12, have been located, in which TS7, TS8, and TS9 derive from 1+*asym*-N_2O_3, while TS10, TS11, and TS12 are formed by 1+*sym*-N_2O_3. For the nitrosations by *asym*-N_2O_3, transition states TS7 and TS8 proceed via direct C-nitrosation (path a), in which there is a replacement of malononitrile methylene hydrogen atom by the nitroso group of *asym*-N_2O_3, leading to the formation of 2+HNO_2 and 2+*trans*-HONO, respectively. The B3LYP barrier heights for TS7 and TS8 in the gas phase are 51.5 and 39.0 kcalmol^{-1}, respectively, which are in good agreement with the barriers of 49.2 kcalmol^{-1} for TS7 and 41.4 kcalmol^{-1} for TS8 at the MP2 level. The barrier height difference between TS7 and TS8 seems most likely due to the strained four-membered ring formed in TS7 with respect to the less strained five-membered ring formed in TS8. For N-nitrosation by *asym*-N_2O_3 (path b), transition state TS9 was located via an activation barrier of 40.5 (33.0) kcalmol^{-1} in the gas phase at the MP2/cc-pVDZ (B3LYP/cc-pVTZ) level, which is lower than those of the C-nitrosation transition states TS7 and TS8. The calculated NPA charges

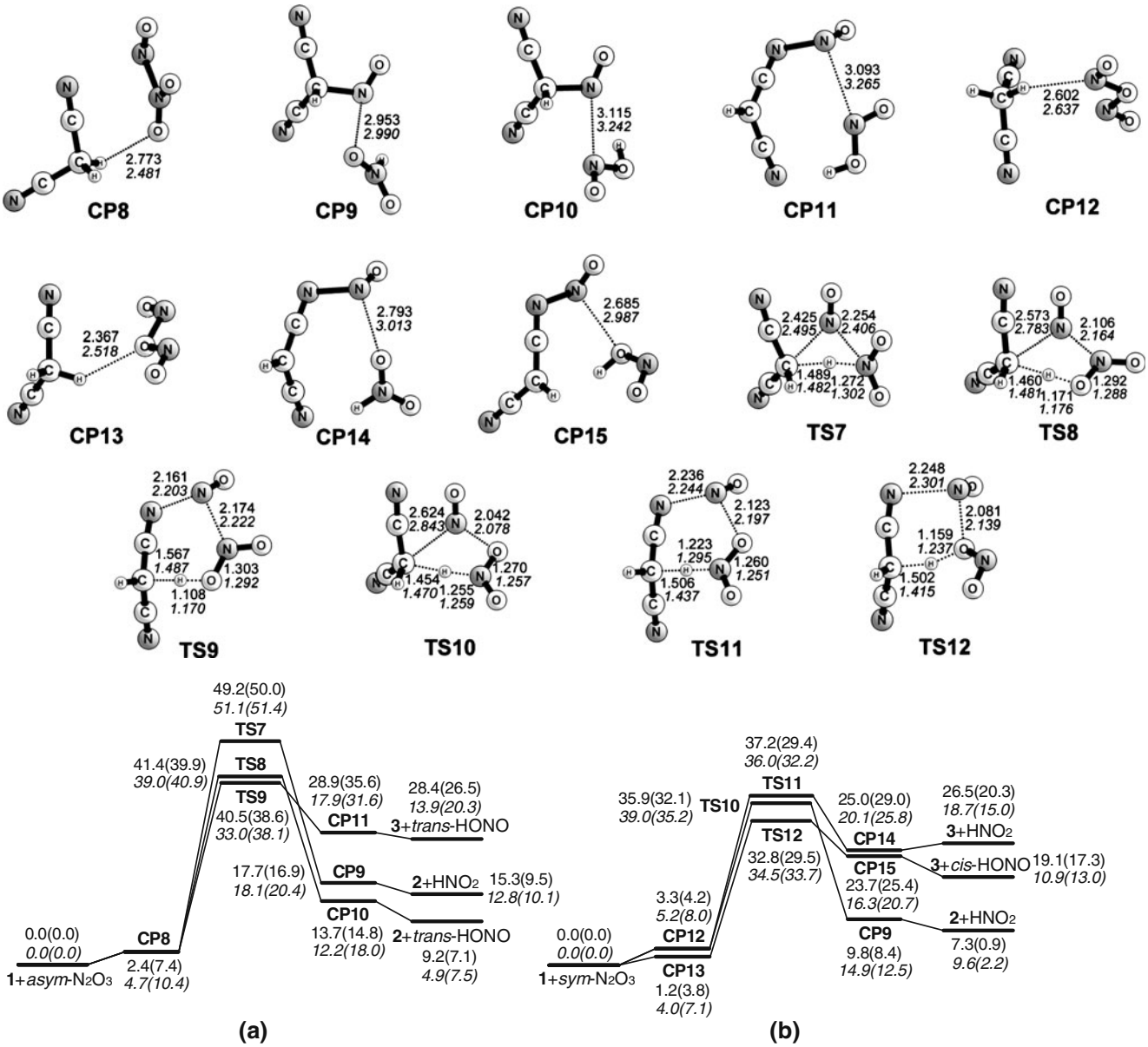

Fig. 6 Optimized geometries (bond lengths in angstroms) of the transition states, the reactant and product complexes and free energy profiles (in kcalmol^{-1}) for the nitrosation of malononitrile, 1, by N_2O_3 in the gas phase at the MP2/cc-pVDZ (numbers in regular form) and B3LYP/cc-pVTZ (numbers in italics) levels. Numbers in parentheses are the relative free energies in water solvent

for the transferred H in TS7~TS9 range from 0.394 to 0.532, the largest value is found for TS9, and the lowest one is for TS7, suggesting proton transfers in these reactions. Solvent effect appears to have little influence over the activation barriers of the nitrosations of malononitrile by *asym*-N_2O_3, which causes the changes in the barriers by 0.3~5.1 kcalmol^{-1}.

For the nitrosations by *sym*-N_2O_3, transition states TS11~TS12 have activation barriers of 32.8~37.2 kcal mol^{-1} in the gas phase at the MP2/cc-pVDZ level, all of which are lower in energy relative to those for the nitrosations by *asym*-N_2O_3. The barriers obtained at the B3LYP/cc-pVTZ level for transition states TS11~TS12 range from 34.5 to 39.0 kcalmol^{-1}, similar to those predicted at the MP2/cc-pVDZ level. The NPA charges for transferred H in TS10, TS11, and TS12 are predicted to be 0.425, 0.440, and 0.511, respectively. Therefore, all of these H transfers are also proton transfers. Inclusion of solvent effect is shown to have a favorable influence on the reaction barriers for the nitrosations by *sym*-N_2O_3, which decreases the activation barriers at both the MP2 and B3LYP levels. On the other hand, solvent effect also changes the stabilization order of the three transition states. In the gas phase, TS12, which is an N-nitrosation transition state, is predicted to have the lowest activation barrier. However, when solvent effect is included, TS11, the other N-nitrosation transition state, becomes the lowest-barrier transition state, lying 29.4 and 32.2 kcalmol^{-1} above 1+ *sym*-N_2O_3 at. MP2/cc-pVDZ and B3LYP/cc-pVTZ levels, respectively. Therefore, the same clear energetic preference for the N-nitrosation mechanism is also predicted for the nitrosations by *sym*-N_2O_3 in aqueous solution.

To determine whether a water molecule could serve as catalyst to accelerate the nitrosation of malononitrile by N_2O_3, we performed analogous water-assisted calculations. The optimized geometries of the transition states, the reactant and product complexes of each channel and the energetics are presented in Fig. 7. The inclusion of the additional water molecule does not have a substantive effect on the gas phase barriers of the six transition states. At the MP2/cc-pVDZ level, the activation barriers of TS8′ and TS9′ are slightly decreased relative to their corresponding non-assisted transition states, and the activation barriers of the other four transition states become a little bit higher. At the B3LYP/cc-pVTZ level, the activation barriers of all six water-assisted transition states are larger than the reactions without the assistance of a water molecule. When the effect of water solvent, in which the experiment was conducted, is also taken into account, the activation barriers of all six transition states increase by 5.4~11.0 kcalmol^{-1} relative to their corresponding non-assisted reactions in solvent at the MP2 level and by 6.6~10.4 kcalmol^{-1} at the B3LYP level. Thus, our calculations reveal that nitrosation of malononitrile by N_2O_3 in aqueous solution proceeds via a nonwater-assisted mechanism, similar to the nitrosations by HONO and ClNO.

N to C nitroso transfer and comparison of the nitrosating activity of the three nitrosating agents

Following the N-nitrosation, a subsequent N → C nitroso transfer occurs in path b to transform the N-nitroso species, 3 to the thermodynamically favored C-nitroso species, 2 (Scheme 1). This intramolecular nitroso transfer is quite facile with a free energy barrier of only 2.4 kcalmol^{-1} in the gas phase or 1.6 kcalmol^{-1} in water solvent at the MP2 level (Fig. 8). The B3LYP also predicts a low barrier of 7.1 (4.4) kcalmol^{-1} in the gas phase (in water solvent). This indicates that the N-nitrosation is the rate-determining step for path b. Taking together the results for the nitrosations by all three nitrosating agents, and comparing the energetic barriers for the rate-determining transition states of both mechanistic nitrosation paths a and b, our calculations predict that although path b is a stepwise pathway via N-nitrosation and N to C nitroso transfer, it is kinetically more preferred than the concerted path a for nitrosations by HONO and N_2O_3 at both MP2/cc-pVDZ and B3LYP/cc-pVTZ levels. In the case of ClNO, the B3LYP also predicts the preference of path b, while nearly equal activation barriers are obtained for both N- and C-nitrosation mechanisms at the MP2 level, suggesting almost identical preference for both paths.

To investigate the nitrosating activity of the three nitrosating agents in the experimental reaction condition, we compared the lowest activation free energy barriers in water solvent for nitrosations by the three nitrosating agents, and both water-assisted and non-assisted reactions are considered (Fig. 9). At the MP2/cc-pVDZ level, the lowest barrier heights of the non-assisted reactions range from 29.4 kcal mol^{-1} to 37.3 kcalmol^{-1} with N_2O_3 being the lowest one and ClNO being the highest one. When the assistance of a water molecule is introduced, the lowest barrier heights increase for all three nitrosating agents, though the stabilization order remains unchanged. The B3LYP/cc-pVTZ calculations predict similar results. Without the assistance of the water molecule, nitrosations by N_2O_3 and ClNO present the lowest (32.2 kcalmol^{-1}) and the highest (38.5 kcalmol^{-1}) barriers, respectively. Introducing an assistant water molecule increases all three barriers by 5.3~9.6 kcalmol^{-1}. These results suggest that nitrosation of malononitrile is a nonwater-assisted process in the aqueous environment, and N_2O_3 is probably the main nitrosating agent.

Intramolecular transformation of 2-nitroso-malononitrile to malononitrileoxime

Once the C-nitroso species 2-nitroso-malononitrile, 2, is formed, it transforms via intramolecular H transfer to the

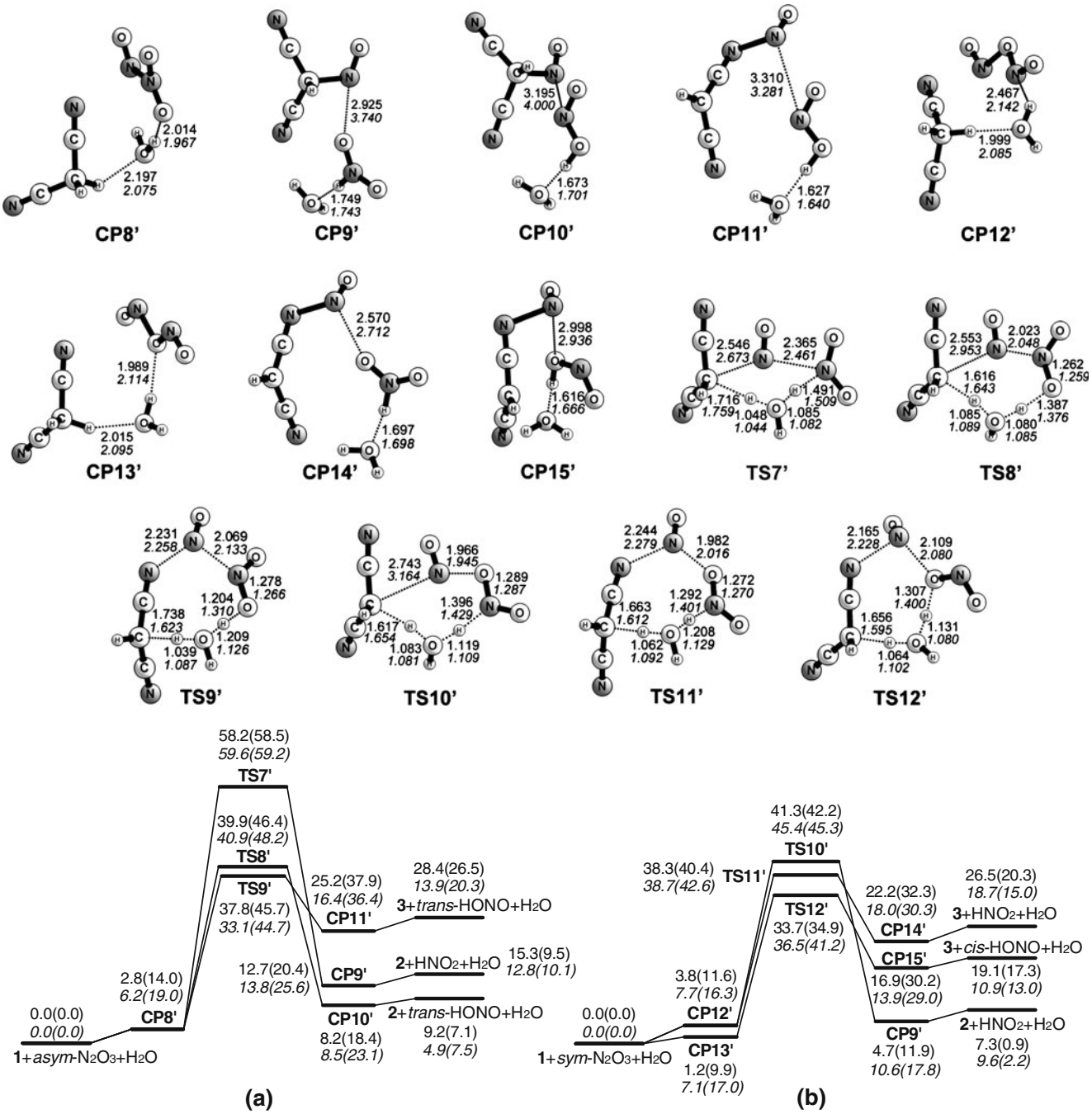

Fig. 7 Optimized geometries (bond lengths in angstroms) of the transition states, the reactant and product complexes and free energy profiles (in kcalmol^{-1}) for the water-assisted nitrosation of malononitrile, 1, by N_2O_3 in the gas phase at the MP2/cc-pVDZ (numbers in regular form) and B3LYP/cc-pVTZ (numbers in italics) levels. Numbers in parentheses are the relative free energies in water solvent

oxime species, malononitrileoxime (4), which is the experimentally observed nitrosating product of malononitrile [9–11]. The H transfer transition state TS14 (Fig. 10) involves a four-membered ring and leads to the generation of malononitrileoxime, 4a, where the CNOH chain is in *cis* form. Relatively strong positive charge of 0.511 is found for the transferred H by NPA calculation, indicating this is more like a proton transfer rather than a hydrogen transfer. The activation free energy barrier for this transformation is predicted to be rather high in the gas phase at both the MP2/cc-pVDZ (57.5 kcalmol^{-1}) and B3LYP/cc-pVTZ (56.0 kcalmol^{-1}) levels, and solvent effect is found to slightly influence the barrier within 1 kcalmol^{-1}.

Since barriers that involve proton transfer can be considerably lowered by adding a water molecule [40–46], the assistance of an explicit water molecule for the reaction was

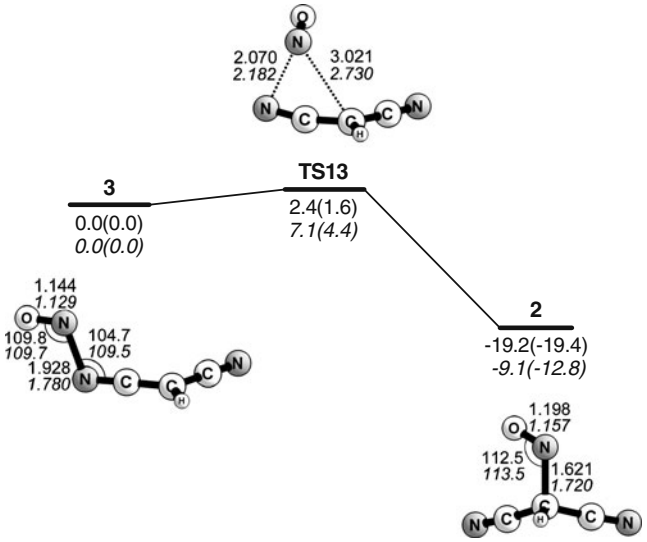

Fig. 8 Free energy profile for the nitroso transfer of N-nitroso species, 3, to 2-nitroso-malononitrile, 2, in the gas phase (in kcalmol^{-1}) at the MP2/cc-pVDZ (numbers in regular form) and B3LYP/cc-pVTZ (numbers in italics) levels. Numbers in parentheses are the relative free energies in water solvent

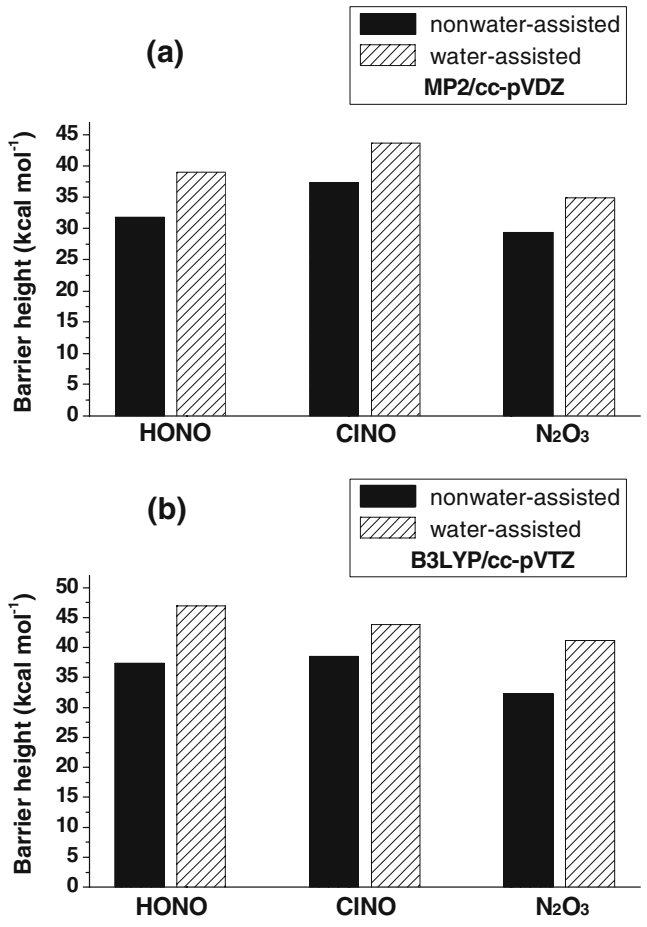

Fig. 9 Lowest free energy barrier heights for nonwater-assisted and water-assisted nitrosations of malononitrile, 1, by each nitrosating agent in water solvent at the (**a**) MP2/cc-pVDZ and (**b**) B3LYP/cc-pVTZ levels

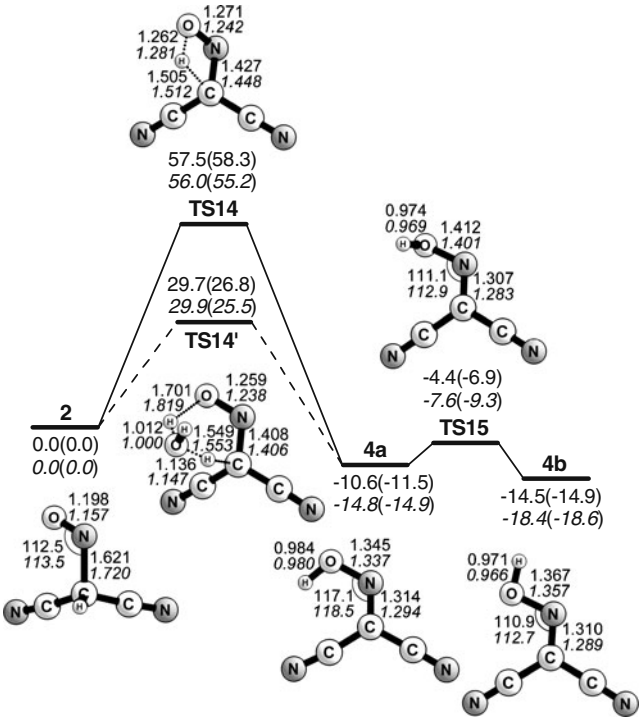

Fig. 10 Free energy profile for the transformation of 2-nitroso-malononitrile, 2, to malononitrileoxime, 4, in the gas phase (in kcalmol^{-1}) at the MP2/cc-pVDZ (numbers in regular form) and B3LYP/cc-pVTZ (numbers in italics) levels. Numbers in parentheses are the relative free energies in water solvent

considered here. As shown in Fig. 10, with the assistance of a water molecule (TS14′), the barrier of the proton transfer drops drastically to 29.9 kcalmol^{-1} in the gas phase at the B3LYP level, in good agreement with the barrier (29.7 kcalmol^{-1}) obtained at the MP2 level. This energetic effect on the barrier via addition of a water molecule can also be ascribed to the relief of the ring strain. When no water molecule is added, the proton transfer proceeds through a strained four-membered ring transition state (TS14), while inclusion of an assistant water molecule extends the transition state to a less strained six-membered ring structure (TS14′), which significantly reduces the energy barrier. Therefore, our calculation strongly supports a water-assisted mechanism in this proton transfer process. Subsequently, the *cis* form malononitrileoxime, 4a, may undergo tautomerization via TS15, where the hydrogen atom rotates around the N-O bond, to form the more stable *trans* isomer, 4b. This rotation proceeds over a moderate barrier of 6.2 (7.2) kcalmol^{-1}, and the final *trans*-malononitrileoxime, 4b, is 3.9 (3.6) kcalmol^{-1} lower in energy than the *cis* isomer, 4a at the MP2/cc-pVDZ (B3LYP/cc-pVTZ) level. The overall transformation is exothermic by 14.5 kcalmol^{-1} in the gas phase and 14.9 kcalmol^{-1} in solvent at the MP2/cc-pVDZ level, and the B3LYP calculation predicts a little bit larger exothermicity of 18.4 and 18.6 kcalmol^{-1} in the gas phase and in water solvent, respectively, indicating the

thermodynamical preference of malononitrileoxime over 2-nitroso-malononitrile.

Conclusions

We have theoretically examined two possible paths for the nitrosation of malononitrile by three nitrosating agents (HONO, ClNO, and N_2O_3) to form 2-nitroso-malononitrile at the MP2/cc-pVDZ and B3LYP/cc-pVTZ levels. The indirect nitrosation path involves N-nitrosation followed by N → C nitroso group transfer. The N-nitrosation is the rate-determining step, while the nitroso transfer is very facile, which requires a barrier of only 2.4 (7.1) kcalmol^{-1} in the gas phase at the MP2/cc-pVDZ (B3LYP/cc-pVTZ) level and an even lower barrier of 1.6 (4.4) kcalmol^{-1} in the experimental condition of aqueous solution. This indirect path is calculated to be more preferred than the direct C-nitrosation path for the nitrosations by HONO and N_2O_3. The origin of the lower energy demand of the N-nitrosation with respect to the C-nitrosation is mainly attributable to the reduction in ring strain of the transition state for the former reaction. Whereas in the case of ClNO, the MP2/cc-pVDZ calculations give almost equal activation barriers for both C- and N-nitrosations, while the B3LYP/cc-pVTZ calculations still prefer the N-nitrosation. Introducing an assistant water molecule does not have a favorable effect on the nitrosations by any of the three nitrosating agents in aqueous solution. Comparing the nitrosating activity of these three nitrosating agent predicts that nitrosation of malononitrile in aqueous occurs with N_2O_3 as the main nitrosating agent. The presence of a water molecule is found to act as a catalyst to substantially reduce the activation barrier of the intramolecular proton transfer from 2-nitroso-malononitrile to malononitrileoxime, which is the resulting observed species of the nitrosation of malononitrile.

Acknowledgments The authors thank the National Key Basic Research Special Foundation of China (Grant No. 2007CB815202) and the National Natural Science Foundation of China (Grant Nos. 20721004 and 20833008) for financial support.

References

1. Turney TA, Wright GA (1959) Nitrous acid and nitrosation. Chem Rev 59:497–513
2. Mirvish SS (1995) Role of *N*-nitroso compounds (NOC) and *N*-nitrosation in etiology of gastric, esophageal, nasopharyngeal and bladder cancer and contribution to cancer of known exposures to NOC. Cancer Lett 93:17–48
3. da Silva G, Kennedy EM, Dlugogorski BZ (2005) Effect of added nucleophilic species on the rate of primary amino acid nitrosation. J Am Chem Soc 127:3664–3665
4. Wu H, Loeppky RN, Glaser R (2005) Nitrosation chemistry of pyrroline, 2-imidazoline, and 2-oxazoline: Theoretical Curtin-Hammett analysis of retro-ene and solvent-assisted C-X cleavage reactions of α-hydroxy-*N*-nitrosamines. J Org Chem 70:6790–6801
5. Freeman F (1969) The chemistry of malononitrile. Chem Rev 69:591–624
6. Motokura K, Fujita N, Mori K, Mizugaki T, Ebitani K, Kaneda K (2005) An acidic layered clay is combined with a basic layered clay for one-pot sequential reactions. J Am Chem Soc 127:9674–9675
7. Costa M, Areias F, Abrunhosa L, Venâncio A, Proença F (2008) The condensation of salicylaldehydes and malononitrile revisited: Synthesis of new dimeric chromene derivatives. J Org Chem 73:1954–1962
8. Elinson MN, Feducovich SK, Stepanov NO, Vereshchagin AN, Nikishin GI (2008) A new strategy of the chemical route to the cyclopropane structure: Direct transformation of benzylidenemalononitriles and malononitrile into 1, 1, 2, 2-tetracyanocyclopropanes. Tetrahedron 64:708–713
9. Longo G (1931) Ricerche sulle diossime LXXVIII. Gazz Chim Ital 61:575–583
10. Iglesias E, Williams DLH (1989) Carbanion nitrosation. Reaction of malononitrile with nitrous acid. J Chem Soc Perkin Trans 2:343–346
11. Andrianov VG (1997) Synthesis and properties of derivatives of 4-aminofuroxan-3-carboxylic acid. Chem Heterocycl Compd 33:973–976
12. Arulsamy N, Bohle DS (2000) Nucleophilic addition of hydroxylamine, methoxylamine, and hydrazine to malononitrileoxime. J Org Chem 65:1139–1143
13. Ichikawa T, Kato T, Takenishi T (1965) A new synthesis of adenine and 4-aminoimidazole-5-carboxamide. J Heterocycl Chem 2:253–255
14. Lu X, Park J, Lin MC (2000) Gas phase reactions of HONO with NO_2, O_3, and HCl: Ab initio and TST study. J Phys Chem A 104:8730–8738
15. Mebel AM, Lin MC, Melius CF (1998) Rate constant of the HONO + HONO → H_2O + NO + NO_2 reaction from ab initio MO and TST calculations. J Phys Chem A 102:1803–1807
16. Li J, Li S (2008) A DFT study toward understanding the high activity of Fe-exchanged zeolites for the "fast" selective catalytic reduction of nitrogen Oxides with ammonia. J Phys Chem C 112:16938–16944
17. Becke AD (1993) Density-functional thermochemistry. III. The role of exact exchange. J Chem Phys 98:5648–5652
18. Lee C, Yang W, Parr RG (1988) Development of the Colle-Salvetti correlation-energy formula into a functional of the electron density. Phys Rev B 37:785–789
19. Dunning TH Jr (1989) Gaussian basis sets for use in correlated molecular calculations. I. The atoms boron through neon and hydrogen. J Chem Phys 90:1007–1023
20. Woon DE, Dunning TH Jr (1993) Gaussian basis sets for use in correlated molecular calculations. III. The atoms aluminum through argon. J Chem Phys 98:1358–1371
21. Møller C, Plesset MS (1934) Note on an approximation treatment for many-electron systems. Phys Rev 46:618–622
22. Frisch MJ, Trucks GW, Schlegel HB, Scuseria GE, Robb MA, Cheeseman JR, Montgomery JA Jr, Vreven T, Kudin KN, Burant JC, Millam JM, Iyengar SS, Tomasi J, Barone V, Mennucci B, Cossi M, Scalmani G, Rega N, Petersson GA, Nakatsuji H, Hada M, Ehara M, Toyota K, Fukuda R, Hasegawa J, Ishida M, Nakajima T, Honda Y, Kitao O, Nakai H, Klene M, Li X, Knox JE, Hratchian HP, Cross JB, Bakken V, Adamo C, Jaramillo J, Gomperts R, Stratmann RE, Yazyev O, Austin AJ, Cammi R, Pomelli C, Ochterski JW, Ayala PY, Morokuma K, Voth GA,

Salvador P, Dannenberg JJ, Zakrzewski VG, Dapprich S, Daniels AD, Strain MC, Farkas O, Malick DK, Rabuck AD, Raghavachari K, Foresman JB, Ortiz JV, Cui Q, Baboul AG, Clifford S, Cioslowski J, Stefanov BB, Liu G, Liashenko A, Piskorz P, Komaromi I, Martin RL, Fox DJ, Keith T, Al-Laham MA, Peng CY, Nanayakkara A, Challacombe M, Gill PMW, Johnson B, Chen W, Wong MW, Gonzalez C, Pople JA (2004) Gaussian 03 Revision D.01. Gaussian Inc, Wallingford, CT

23. Gonzalez C, Schlegel HB (1989) An improved algorithm for reaction path following. J Chem Phys 90:2154–2161
24. Gonzalez C, Schlegel HB (1990) Reaction path following in mass-weighted internal coordinates. J Phys Chem 94:5523–5527
25. Foster JP, Weinhold F (1980) Natural hybrid orbitals. J Am Chem Soc 102:7211–7218
26. Reed AE, Weinhold F (1983) Natural bond orbital analysis of near-Hartree-Fock water dimer. J Chem Phys 78:4066–4073
27. Reed AE, Weinhold F (1985) Natural localized molecular orbitals. J Chem Phys 83:1736–1740
28. Reed AE, Weinstock RB, Weinhold F (1985) Natural population analysis. J Chem Phys 83:735–746
29. Reed AE, Curtiss LA, Weinhold F (1988) Intermolecular interactions from a natural bond orbital, donor-acceptor viewpoint. Chem Rev 88:899–926
30. Glendening ED, Reed AE, Carpenter JE, Weinhold F NBO Version 3.1
31. Tomasi J, Persico M (1994) Molecular interactions in solution: An overview of methods based on continuous distributions of the solvent. Chem Rev 94:2027–2094
32. Chu TS, Zhang Y, Han KL (2006) The time-dependent quantum wave packet approach to the electronically nonadiabatic processes in chemical reactions. Int Rev Phys Chem 25:201–235
33. Xie TX, Zhang Y, Zhao MY, Han KL (2003) Calculations of the F + HD reaction on three potential energy surface. Phys Chem Chem Phys 5:2034–2038
34. Chu TS, Han KL (2008) Effect of Coriolis coupling in chemical reaction dynamics. Phys Chem Chem Phys 10:2431–2441
35. Han KL, He GZ (2007) Photochemistry of aryl halides: Photodissociation dynamics. J Photoch Photobio C Rev 8:55–66
36. Chu TS, Han KL (2005) Nonadiabatic time-dependent wave packet study of $D^{+}+H_2$ reaction system. J Phys Chem A 109:2050–2056
37. McQuaid MJ, Ishikawa Y (2006) H-atom abstraction from CH3NHNH2 by NO2: CCSD(T)/6–311++G(3df, 2p)//MPWB1K/6–31+G(d, p) and CCSD(T)/6–311+G(2df, p)//CCSD/6–31+G(d, p) calculations. J Phys Chem A 110:6129–6138
38. Varetti EL, Pimentel GC (1971) Isomeric forms of dinitrogen trioxide in a nitrogen matrix. J Chem Phys 55:3813–3821
39. Nour EM, Chen LH, Laane J (1983) Interconversion studies and characterization of asymmetric and symmetric dinitrogen trioxide in nitric oxide matrixes by Raman and infrared spectroscopy. J Phys Chem 87:1113–1120
40. Tavakol H, Arshadi S (2009) Theoretical investigation of tautomerism in N-hydroxy amidines. J Mol Model 15:807–816
41. Li J, Wang GP, Schlegel HB (2006) A computational exploration of some transnitrosation and thiolation reactions involving CH_3SNO, CH_3ONO and CH_3NHNO. Org Biomol Chem 4:1352–1364
42. Wang Y, Kumar D, Yang C, Han K, Shaik S (2007) Theoretical study of N-demethylation of substituted N, N-dimethylanilines by cytochrome P450: The mechanistic significance of kinetic isotope effect profiles. J Phys Chem B 111:7700–7710
43. Munk BH, Burrows CJ, Schlegel HB (2008) An exploration of mechanisms for the transformation of 8-oxoguanine to guanidinohydantoin and spiroiminodihydantoin by density functional theory. J Am Chem Soc 130:5245–5256
44. Wang HM, Wang Y, Han KL, Peng XJ (2005) A DFT study of Diels-Alder reactions of o-quinone methides and various substituted ethenes: Selectivity and reaction mechanism. J Org Chem 70:4910–4917
45. Li J, Jiang WY, Han KL, He GZ, Li C (2003) Density functional study on the mechanism of bicyclic guanidine-catalyzed Strecker reaction. J Org Chem 68:8786–8789
46. Song GY, Su Y, Periana RA, Crabtree RH, Han KL, Zhang HJ, Li XW (2010) Anion-Exchange-Triggered 1, 3-shift of an NH proton to iridium in protic N-heterocyclic carbenes: hydrogen-bonding and ion-pairing effects. Angew Chem Int Ed 49:912–917